Computational analysis method of local electrical conductive property in nano-size materials

Cite as: AIP Advances **9**, 025106 (2019); https://doi.org/10.1063/1.5085360
Submitted: 11 December 2018 . Accepted: 01 February 2019 . Published Online: 11 February 2019

Masato Senami, Makoto Nakanishi, and Akitomo Tachibana

Computational analysis method of local electrical conductive property in nano-size materials

Cite as: AIP Advances 9, 025106 (2019); doi: 10.1063/1.5085360
Submitted: 11 December 2018 • Accepted: 1 February 2019 •
Published Online: 11 February 2019

Masato Senami,[a] Makoto Nakanishi, and Akitomo Tachibana

AFFILIATIONS

Department of Micro Engineering, Kyoto University, Kyoto 615-8540, Japan

[a]Electronic mail: senami@me.kyoto-u.ac.jp

ABSTRACT

Two new local conductance quantities are studied. The ordinary global conductance may not be appropriate for the study of nanosize materials, while our new local conductance quantities have an advantage for the study of these materials. Graphene is chosen as a nano-material example for our study since graphene has a simple conduction property. The integrated value of our local conductances are compared to the conductance of the Landauer formula. The local conductances in various local regions in graphene sheet are studied, and it is demonstrated that our local conductances have good properties for the analysis of nanosize materials.

I. INTRODUCTION

Recently, semiconductor devices have downsized significantly owing to the progress of technology. Nano-devices such as single molecule transistor become more important for creating next-generation semiconductor devices. In the electrical conduction in these nanosize materials, the classical Ohm's law is not so good law compared to that in macroscopic phenomena, since quantum effects such as quantized conductance appear. Many studies of electrical conduction based on quantum mechanics, which is represented by the Landauer formula,[1] are reported. We consider that the analysis based on quantum mechanics is a good way but not the best for electrical conduction in nano-devices. QED (Quantum ElectroDynamics), which is one of quantum field theory, is known as more precise and correct theory than quantum mechanics. In QED, the electromagnetic field is consistent with Maxwell's equations. In addition, QED is consistent with special relativity.

As a result, we consider that QED is a better tool for the study of dynamic phenomena such as electrical conduction. Electronic structure computations fully based on QED is not available yet, although some challenge is progressing.[2–5] Hence, we could not study electrical conduction phenomena fully based on QED. However, some local physical quantities have been proposed based on QED.[6,7] These are local dielectric constant,[8] local electrical conductivity,[9,10] local spin torque[11] and so on. These quantities have been shown to have some advantages over ordinary macroscopic quantities. In nanosize materials, physical quantities are known to have strong position dependence and are considered to be strongly affected by defects, impurities, and interfaces. For example, gate leakage current in dielectric thin films depends on a position in materials.[12] Hence, ordinary macroscopic and averaged quantities are considered not to be suitable for the study of these nano-materials. For example, the analysis of leakage current by using ordinary macroscopic conductivities clarifies the effects of impurities only indirectly.

For the study of quantum local electrical conductive properties of nanomaterials, local electrical conductivity tensor has been proposed in our group. This tensor represents the relation between electric field and local current density, and shows us the dependence of electrical conductive properties in a local region. In our previous works,[9,10] nanowire materials of silicon and GaN were studied by these local electrical conductivity tensor. However, we did not have a method to compare our local conductivity and ordinary conduction quantity. In the present study, we study a method of

comparing our conductivity with other established quantity. For this purpose, we propose the calculation of local electrical conductance quantities from local electric current density. We suggest two definitions of local electrical conductance in the first trial. We study the behavior of local electrical conduction for graphene sheet by local electrical conductance with the wave packet derived by computations based on quantum mechanics. Although we use this wave packet, we can partially reveal physical property about electrical conduction by using local quantities based on quantum field theory as our previous works. Particularly, we compare our conductance with the conductance value based on the Landauer formula.[1] We discuss the characteristics of local electrical conduction with this new quantity, and clarify how local quantities represent electrical conduction phenomena.

II. THEORY

In this section, we introduce our local physical quantities.[6,7] Our local electrical conductivity tensor operator $\hat{\overleftrightarrow{\sigma}}$ is defined as follows,[7]

$$\hat{\vec{j}}(\vec{r}) = \hat{\overleftrightarrow{\sigma}}_{\mathrm{ext}}(\vec{r})\hat{\vec{D}}(\vec{r}), \tag{1}$$

where $\hat{\vec{j}}(\vec{r})$ is local electric current density operator and $\hat{\vec{D}}(\vec{r})$ is electric displacement field operator, which is considered to be external electric field. The current density operator, $\hat{\vec{j}}(\vec{r})$, is defined as

$$\hat{\vec{j}}(\vec{r}) = \frac{1}{2}\left[i\hbar\hat{\Psi}^{\dagger}(\vec{r})\vec{\nabla}\hat{\Psi}(\vec{r}) - \frac{1}{c}\hat{\Psi}^{\dagger}(\vec{r})\hat{\vec{A}}(\vec{r})\hat{\Psi}(\vec{r}) + h.c.\right], \tag{2}$$

where $\hbar$ is the reduced Planck constant, c is the speed of light in the vacuum, and $\hat{\vec{A}}$ is vector potential operator. The relation between operators,

$$\hat{\vec{D}}(\vec{r}) = \hat{\overleftrightarrow{\epsilon}}(\vec{r})\hat{\vec{E}}(\vec{r}), \tag{3}$$

where $\hat{\vec{E}}(\vec{r})$ is electric field operator, defines local dielectric constant tensor operator, $\hat{\overleftrightarrow{\epsilon}}(\vec{r})$,[8] which is the local counterpart of dielectric constant tensor. With this relation, local internal electrical conductivity tensor operator, $\hat{\overleftrightarrow{\sigma}}_{\mathrm{int}}(\vec{r})$, can be defined as

$$\hat{\vec{j}}(\vec{r}) = \hat{\overleftrightarrow{\sigma}}_{\mathrm{ext}}(\vec{r})\hat{\overleftrightarrow{\epsilon}}(\vec{r})\hat{\vec{E}}(\vec{r}) = \hat{\overleftrightarrow{\sigma}}_{\mathrm{int}}(\vec{r})\hat{\vec{E}}(\vec{r}). \tag{4}$$

Local internal conductivity tensor shows the relation between internal electric field in a matter and current density and how the electric field at a position in a matter drives electrical carriers. This effect is only studied from microscopic points of view and does not have the corresponding macroscopic quantity. This internal conductivity tensor has been studied in our previous works.[10] In the present work, local internal conductivity tensor is not studied and only local external conductivity is paid attention to.

We have proposed the local conductivity as a new quantity. In a viewpoint of the check of the relation of our local conductivity and ordinary quantities of conduction, our local conductivity is not directly compared to observed or computed conductance. Hence for the comparison with the computed value of ordinary conductance, which is given by the Landauer formula, local conductance is defined in this work. When the region where local conductance is computed is chosen to be the same for the computation of the Landauer formula, we expect that our local conductance shows properties similar to that by the Landauer formula.

The definition of our local conductance is given with local current density. In the following, we use expectation values of operators. Expectation values are derived by sandwiching operators between state vectors, bra and ket. In our notation, we drop bra and ket for expectation values, and we discriminate operators and expectation values by the hat symbol for operators.

We define two local conductances from two different viewpoints of the local current of a region. A box region is assumed in both definitions. Our local conductances are inspired with the ordinary conductance formula,

$$G = I/V_B, \tag{5}$$

where G is the ordinary conductance, I is total current, and V_B is a bias voltage. In this representation, the direction of I is implicitly considered to be the same direction as a bias voltage. In a local region, due to the existence of electric fields by nuclei and electrons as well as one by a bias voltage, the direction of electric current does not coincide with that of a bias voltage exactly, and hence off-diagonal elements in local conductivity tensor (1) are important. However, we neglect these off-diagonal effects in this work for simplicity, because local regions are chosen so that off-diagonal elements are small.

In the first definition (LC1) of local conductance, the total current is chosen to be the average of the whole region of a rectangular box region (Fig. 1(a)). The definition is given as

$$G_{\mathrm{LC1}} = \frac{\frac{1}{L}\int_V j_x(\vec{r})d\vec{r}}{V'_B}, \tag{6}$$

where the direction of a bias voltage is assumed to be x-direction. L is the length of the box region for the direction parallel to that of the bias voltage and V'_B is the bias voltage between ends of the box region, $V'_B = V_B(L/L_{\mathrm{channel}})$, where L_{channel} is the length from the end of the left lead to the end of the right lead in the calculated system, that is, the length of the system applied the bias voltage. Hence V'_B/L is considered to be averaged external electric field for the box region. In this

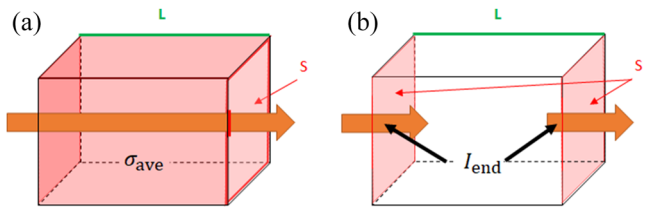

FIG. 1. Scheme of the definition of our local conductance. Panels (a) and (b) shows the first (LC1) and second (LC2) definitions, respectively.

representation, an external electric field is assumed to be uniform in the system and voltage drop is assumed to be linear. This assumption is good for graphene used in our computations and our choice of local regions as shown in later sections. This local conductance can be reduced to the form with local external conductivity instead of current density,

$$G_{LC1} = \frac{\sigma_{ave} S}{L} = \frac{1}{L^2} \int_V \sigma_{ext,\,xx}(\vec{r}) d\vec{r}, \tag{7}$$

where S is the area of cross section of the box region as shown in Fig. 1. The average of the local conductivity, σ_{ave}, in the region is given as

$$\sigma_{ave} = \frac{1}{V} \int_V \sigma_{ext,\,xx}(\vec{r}) d\vec{r}. \tag{8}$$

This relation is inspired by the reduction of the conductance form $I = GV_B$ into the conductivity form

$$\frac{I}{S} = \frac{\sigma_{ave} V'_B}{L}. \tag{9}$$

The second definition (LC2) uses the current of the surfaces at ends of the box region (Fig. 1(b)), I_{end}. I_{end} is calculated from the local current density at ends, and given as

$$I_{end} = \frac{1}{2} \sum_{ends} \int_S j_x(\vec{r}) d^2\vec{r}. \tag{10}$$

Hence, we define the second local conductance as

$$G_{LC2} = \frac{I_{end}}{V'_B}. \tag{11}$$

LC2 is based on the notion of continuous current and is similar to Landauer formula. LC1 is able to analyze even noncontinuous current, such as hopping conduction. Hence both conductances show similar value for good conductor. For organic materials, two conductances are considered to give different results. In this work, we confirm the former property, while the study of the latter one is our future work. The local effect of conductivity is addressed and the primary purpose of this work is the confirmation of our local conductivity by the comparison with other established conductive quantity, the conductance based on the Landauer formula. In our future work, local conductive properties are addressed further.

III. COMPUTATIONAL DETAIL

As mentioned above, our formalism is based on QED, and hence the calculation of state vectors should be performed by an approach based on quantum field theory. However, any computational code based on fully quantum field theory is not available, and hence we use wave functions derived by electronic structure computations based on quantum mechanics as a substitution. In this work, the local current density is required for the evaluation of local conductance, and we should compute conduction states of a target material. For these computations, we adopt non-equilibrium Green function method,[13,14] and OpenMX[15] program package is used for the computations of wave packets, while QEDynamics[5] is used for the computations of our local physical quantities.

In this work, we choose graphene sheet as an example for our study, which is planar structure carbon material. Our computational model of the graphene sheet is shown in Fig. 2. Our graphene model is composed of 24 carbon atoms, and leftmost and rightmost four atoms in the unit cell are considered to be the left and right lead, respectively. It is assumed that outside regions of the leads have the same structure and continues semi-infinitely along x-direction. For y and z-direction, a periodic boundary condition is imposed. For y-direction, the same pattern continues repeatedly as shown in Fig. 2. For z-direction, the cell size is taken to be 18.9 [bohr] so that the effect from next cells can be negligible. The internuclear length between carbon atoms in graphene is 2.68 [bohr]. The basis set for carbon atoms is chosen to be C5.0-s2p1. The numbers of k-points are 30 and 1 for y and z-directions, respectively. In our computations, local density approximation is used as exchange-correlation functional and cutoff energy is 200 [Ry]. In computations of non-equilibrium Green function method, Fermi-Dirac distribution is used for electron ensembles in lead parts. The temperature of this distribution is set to be 600 [K].

For the computation of local conductivity tensor, the approximation, $\vec{j}(\vec{r}) = \overleftrightarrow{\sigma}_{ext}(\vec{r})\vec{D}(\vec{r})$, is adopted. In this work, we assume that a uniform external electrical field, whose value is D_x, is applied to x-direction, which is considered to come from a bias voltage. The finite difference method for the computation of local conductivity is used. In this work, only the xx-component is discussed and differential conductivity is shown. The xx-component of the local conductivity tensor is

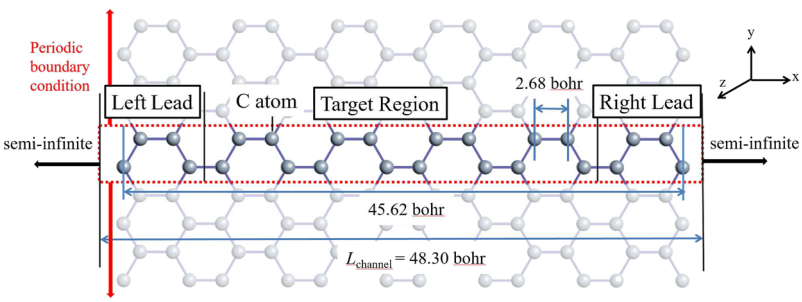

FIG. 2. Our computational model of graphene sheet. "Target Region" is the region for the analysis of local physical quantities, "Left Lead" and "Right Lead" are lead structures and in "semi-infinite" regions, the same structure is repeatedly continued.

computed as

$$\sigma_{\text{ext, xx}}(\vec{r}) = \frac{j_x(\vec{r}; D_x + \Delta D_x) - j_x(\vec{r}; D_x - \Delta D_x)}{2\Delta D_x}, \quad (12)$$

where ΔD_x is chosen to be 0.1 [V]/48.30 [bohr]. The value of ΔD_x is determined by the bias voltage and the distance between leads, L_{channel} = 48.30 [bohr], and the bias voltage is taken from 0.1 [V] to 2.5 [V] by 0.1 [V].

In the computation of current density, the vector potential term is not included, since effects of vector potential are negligible for wave packets derived by calculation based on quantum mechanics with small current density.[16]

In this work, the conductance by the Landauer formula is compared with our conductances. In this computation, we use the following manner for the purpose of the comparison. The current is computed in a viewpoint of the Landauer formula as[17]

$$I_{\text{Landauer}} = \frac{e}{h}\int dE T(E)\Delta f(E), \quad (13)$$

where T is the transmission and $\Delta f(E)$ is the difference of the Fermi-Dirac distribution function between left and right leads. The conductance is calculated from this current by $G = I/V_B$ as

$$G_{\text{Landauer}} = \frac{I_{\text{Landauer}}}{V'_B}. \quad (14)$$

Here we use V'_B instead of V_B. The definition of I_{Landauer} in OpenMX is calculated for the region including the left and right lead denoted in Fig. 2, and the conductance of the Landauer formula is appropriately scaled for the purpose of comparison.

IV. RESULTS

A. Comparison with Landauer formula

First, the total conductance of our model is calculated, and this is for the purpose of the comparison between our conductances and the conductance by the Landauer formula and the confirmation that our local conductances have also good properties of the ordinary global conductance. The total conductance of our model means the conductance for the target region shown in Fig. 2 and the integration range for z direction is taken to be large enough. The total conductance of our model as functions of the bias voltage is shown in Fig. 3. In addition to the two local conductances proposed in this work, the conductance by the Landauer formula is shown. G_{LC1} (G_{LC2}) means the local conductance by the definition LC1 (LC2), and G_{Landauer} is calculated by the Landauer formula as explained in the previous section. As mentioned in the previous section, the computational region of I_{Landauer} is larger than the region of $G_{LC1,2}$. Therefore, G_{Landauer} is scaled as that for the same region, for comparison. All conductances have some common features as seen in Fig. 3. All of the three conductances remain substantially constant from 0.1 [V] to 0.5 [V] and increase monotonically from 0.6 [V] to 2.5 [V]. Thus, our local conductances show similar behavior to G_{Landauer}. It is shown that the value of G_{LC2} is larger than G_{LC1} for the whole range of bias voltage, because the current density is large on the

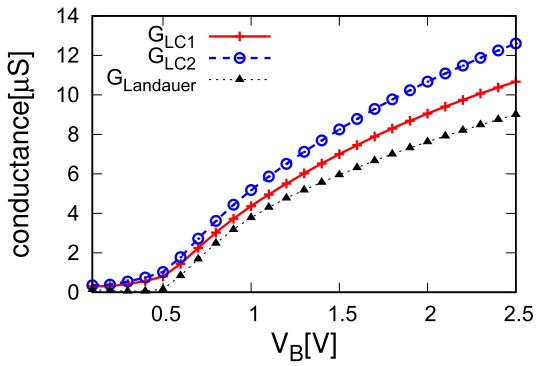

FIG. 3. The total conductance of G_{LC1}, G_{LC2}, and G_{Landauer} as a function of bias voltage.

planes at the ends of the target region as shown later. G_{LC1} is almost the same as G_{Landauer}, while the difference of G_{LC2} from G_{Landauer} is slightly larger than G_{LC1}. The difference between G_{LC2} and G_{Landauer} arises partially from the difference of the current. In Fig. 4, the current, I_{end}, on the plane at the ends of the region and the current, I_{Landauer}, by the Landauer formula are shown as a function of bias voltage. The similar behavior is seen also in the current and it can be seen I_{end} is slightly larger than I_{Landauer}. This difference is speculated to originate in the difference of the evaluation method of current. Particularly, I_{end} is calculated on the plane at the leftmost and rightmost carbon nuclei in the target region, while I_{Landauer} is the transition between the lead and the target region. Therefore, it can be said that our two local conductances have good properties for the representation of conductance as well as the Landauer formula. One of the reasons why tendency of our conductances is similar to G_{Landauer} is that all conductances originate in the equation, $G = I/V_B$.

As shown in this subsection, our local conductance, G_{LC1}, shows close values to the conductance by the Landauer formula. Hence our local conductivity is confirmed to be a

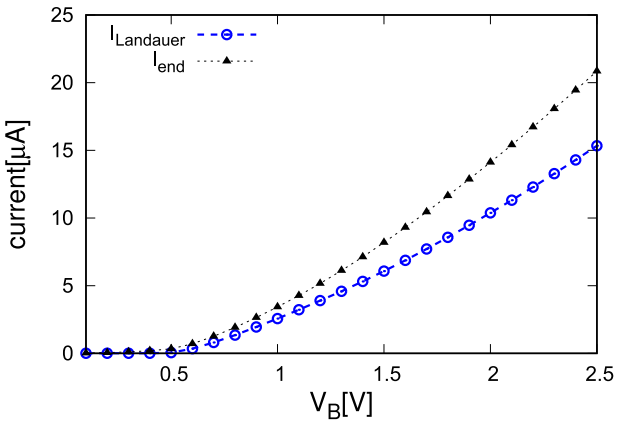

FIG. 4. The currents, I_{end} and I_{Landauer}, are shown as a function of bias voltage.

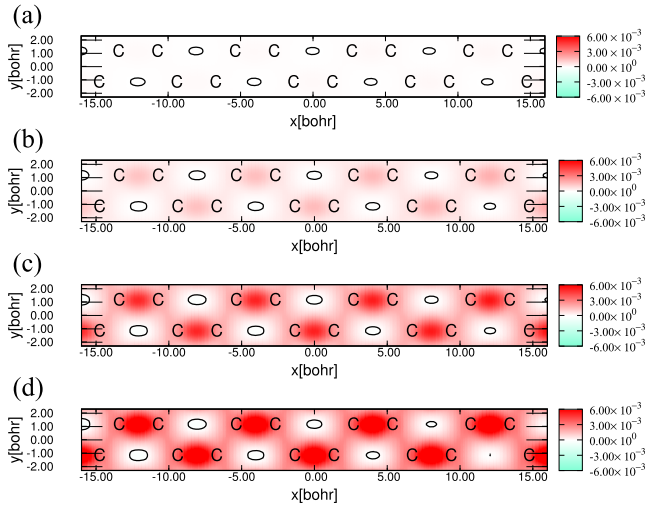

FIG. 5. The distribution of the local conductivity is shown at (a) 0.1 [V], (b) 0.5 [V], (c) 1.0 [V], and (d) 2.0 [V] bias voltages on z = 1.34 [bohr] plane. The mark "C" represents positions of carbon nuclei. The depth of color represents the magnitude of the local conductivity. The local conductivity is zero on solid lines.

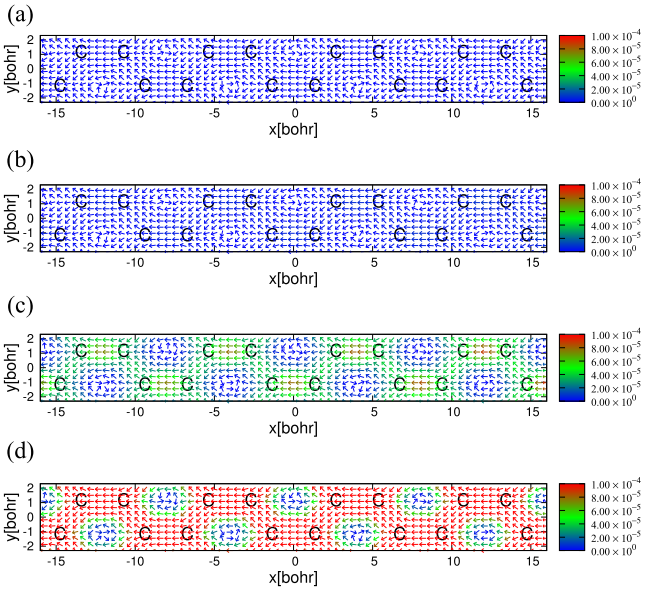

FIG. 6. The distribution of the local current density is shown at 0.1 [V], 0.5 [V], 1.0 [V], and 2.0 [V] on z = 1.34 [bohr] plane. The direction of an arrow represents the direction of $\vec{j}$. The mark "C" represents positions of carbon nuclei. The color represents the magnitude of current density.

reasonable quantity to study the local property of conduction. In addition, our local conductances themselves are good quantities for the study.

B. Local distribution of conductivity and current

Next, we show the distribution of the differential local conductivity, $\sigma_{\text{ext, xx}}(\vec{r})$, on z = 1.34 [bohr] plane at bias voltages, 0.1, 0.5, 1.0, 2.0 [V], in Fig. 5. From these figures, we can see a path of large current density. The current on z = 1.34 [bohr] plane is larger than that on graphene sheet z = 0 due to π-bonding. From this figure, it is shown that the distribution pattern of $\sigma_{\text{ext, xx}}(\vec{r})$ is not changed by a bias voltage. $\sigma_{\text{ext, xx}}(\vec{r})$ is large in the region between two adjacent carbon atoms for x-direction, since the bias voltage is applied to x-direction. $\sigma_{\text{ext, xx}}(\vec{r})$ is very small in the center area of a hexagon of carbon atoms, and hence it is speculated that the current hardly flows in this area.

The distribution of the current density $\vec{j}$ on z = 1.34 [bohr] plane at bias voltages, 0.1, 0.5, 1.0, 2.0 [V], is shown in Fig. 6. The direction of an arrow represents the direction of $\vec{j}$, and thus we can see how the current flows locally in graphene. From this figure, it is shown that the current principally flows through two adjacent carbon atoms, which is reasonably consistent with the distribution of $\sigma_{\text{ext, xx}}(\vec{r})$. In addition, we can see that the current flows like a vortex around the center of hexagons, where the current is small.

Thus, from our local conductivity, we can see various local information such as where the electric current is large locally in materials. Hence we consider that the analysis with the local physical quantities is effective for theoretical analysis.

C. Conductance of local regions in graphene

As one of the advantages of our local conductances, the conductance at a local region can be evaluated. For the demonstration of this analysis, we take local regions shown in Fig. 7 and evaluate local conductances. As a criterion of the size of the local regions, we choose the internuclear distance between carbon atoms, $2L$. For the regions (a)-(g), the local regions are taken as a cube where the length of the side is $2L$. The center positions of the regions (a)-(g) are chosen to be positions of carbon nuclei. For the region (e), (f) and (g), the center positions of the region (e) and (f) are the midpoint between carbon nuclei and the center of the region (g) is the

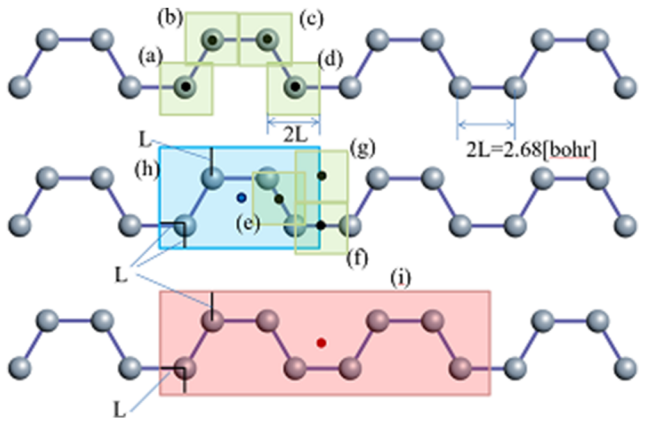

FIG. 7. The choices of box regions. Squares are the cross section of boxes and symmetric for the dot in the center of the square. Boxes are also symmetric for both sides of the graphene sheet. L is the half of the internuclear length between carbon atoms. The local regions with the same color have the same volume of boxes.

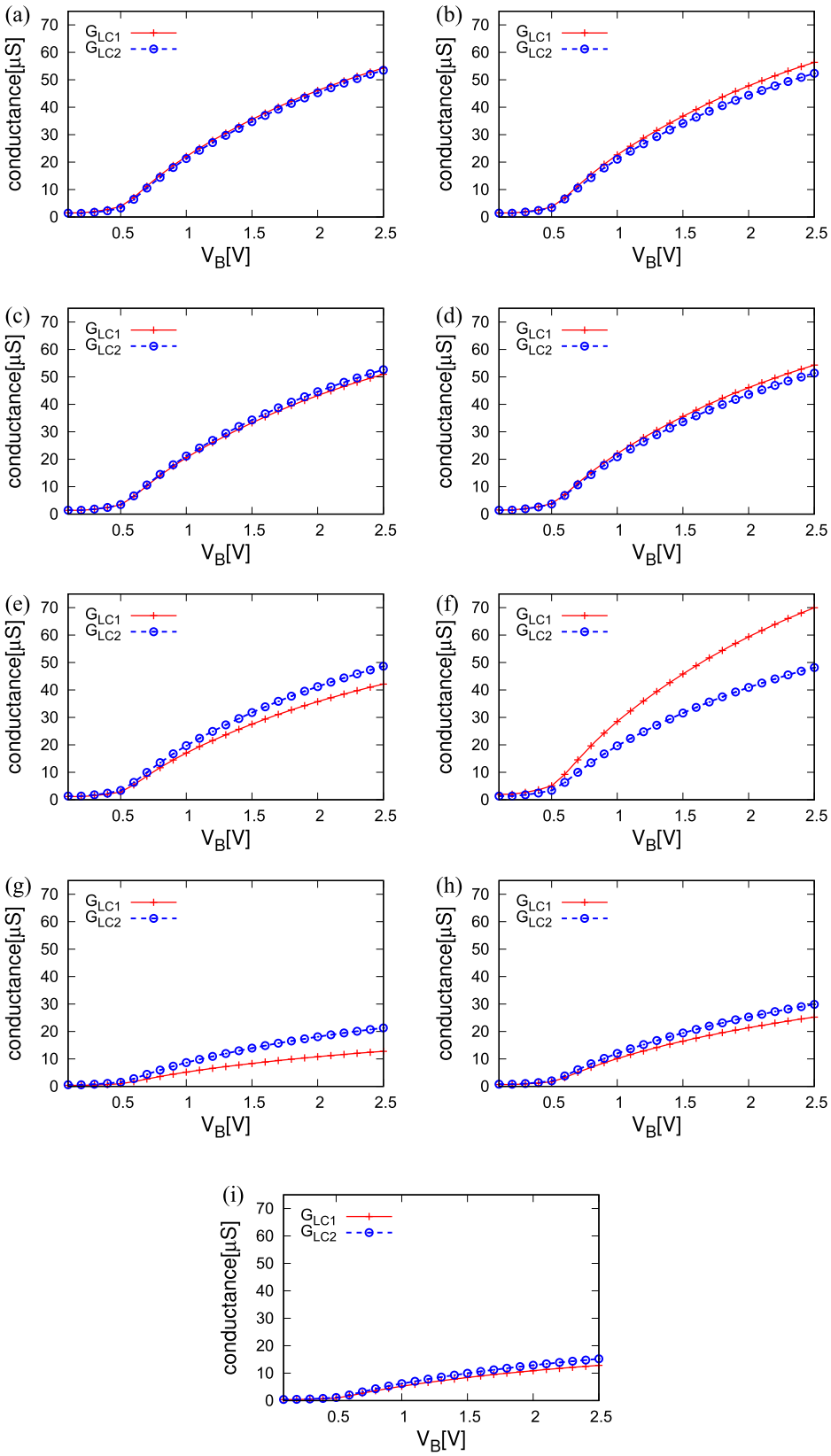

FIG. 8. G_{LC1} and G_{LC2} are shown as the function of the bias voltage. Panels (a)-(i) correspond to the local regions (a)-(i) in Fig. 7, respectively.

center of the hexagon. These center positions are represented as black dots in Fig. 7. In addition, we take two larger regions, the region (h) includes four carbons, and the other region (i) includes eight carbon atoms. The center positions of these regions are represented as a blue dot and a red dot, respectively, and the depth of both boxes is 2L. The local conductances of these regions are shown as functions of bias voltage in Fig. 8. It is seen from this figure that G_{LC1} (G_{LC2}) has almost the same values for the regions (a)-(d) due to a symmetric structure of graphene sheet. The very small difference in these four results arises from the effect of the symmetry breaking for the x-direction due to the existence of the electric current. In Fig. 8, the local conductance of the region (f) is the highest in the regions (a)-(i) for G_{LC1}, which means that the current flow the most largely in the region (f) as shown in Figs. 5 and 6. The value of G_{LC2} of the region (f) is close to those from the regions (a)-(d). Since the conductance of G_{LC2} depends heavily on the choice of a region, particularly the choice of the surfaces, G_{LC2} is not as large as G_{LC1} in the region (f). The value of G_{LC1} in the region (e) is lower than in the region (f), since π-bond exists in the region (f) and not in the region (e). The region (g) has very small conductance for both G_{LC1} and G_{LC2} as speculated from Figs. 5 and 6. From the panels (a)-(g), it can be confirmed that the electric current distribution in the graphene sheet is the largest around π-bond and almost homogeneous in other regions except for the center of the carbon hexagon. Our conductances are dependent on the size of the boxes as ordinary conductance. In Fig. 8(h), the values of conductances are smaller than the regions (a)-(f) as expected. The value of G_{LC1} is almost half of those of the regions (a)-(d). This is because the denominator V'_B is three times as large as that in the regions (a)-(d) and the averaged current is about 1.5 times. The current in the region (h) is roughly estimated to be the sum of those of the regions (a)-(d) and two times that of the region (g), and the length of the region (h) is three times as long as the region (a)-(g). Hence $\frac{1}{L}\int_V j_x(\vec{r})d\vec{r}$ is about 1.5 times. The value of G_{LC2} is slightly larger than half of those of the regions (a)-(d), since both ends of the region (h) include π-bonding where the electric current is the largest. The result of the region (i) is further smaller. This is considered to originate in the size of regions, and hence the values of G_{LC1} and G_{LC2} of the region (i) is about half of that of the region (h). This corresponds to the feature of the ordinary conductance. Note that G_{LC1} and G_{LC2} of the region (i) is not twice as large as the result of the target region shown in Fig. 3. This is because in the computation of G_{LC1} and G_{LC2} in Fig. 3, the range of z-coordinate is much larger than that in the region (i) and the electric current in $|z| > L$ is included. As a result, our local conductances have good properties to analyze in a local region of nanosize materials.

V. SUMMARY

In this work, we have studied two new local conductance quantities based on quantum field theory, which can represent conductance in local regions. Our new local conductances are inspired with the ordinary conductance formula with the local current density. One definition of our local conductance is based on the averaged local current in a target local region, while the other definition is based on the current which flows the ends of a target local region. The former is introduced for the confirmation of local conductivity proposed by our group. For demonstration, graphene is chosen as an example material, and we have shown our local conductances as a function of bias voltage and the distributions of some other local quantities. Our two local conductances have shown similar features to the ordinary conductance based on the Landauer formula. In addition, we have shown that our conductances have advantages over the ordinary conductance for analyzing local region in nanosize materials. In the future, we should develop the analysis method of the electrical conduction in a local region of nanosize materials.

ACKNOWLEDGMENTS

This work was supported in part by a Grant-in-Aid for Scientific Research (C) (17K04982) and Grant for Basic Science Research Projects from The Sumitomo Foundation. The computations were performed in part using Research Center for Computational Science, Okazaki, Japan.

REFERENCES

[1]For example see, Y. V. Nazarov and Y. M. Blanter, *Quantum Transport: Introduction to Nanoscience* Cambridge University Press, (2009) and references therein.

[2]J. Berges, AIP Conf. Proc. **739**, 3 (2005); F. Hebenstreit, J. Berges, and D. Gelfand, Phys. Rev. **D87**, 105006 (2013), and references therein.

[3]U. D. Jentschura, Can. J. Phys. **89**, 109 (2011); U. D. Jentschura and J. Evers, *ibid.* **83**, 375 (2005).

[4]K. D. Lamb, C. C. Gerry, Q. Su, and R. Grobe, Phys. Rev. A **75**, 013425 (2007); R. E. Wagner, M. R. Ware, B. T. Shields, Q. Su, and R. Grobe, Phys. Rev. Lett. **106**, 023601 (2011); R. E. Wagner, Q. Su, and R. Grobe, Phys. Rev. A **88**, 012113 (2013), and references therein.

[5]QEDynamics, M. Senami, K. Ichikawa, and A. Tachibana, https://github.com/mfukudaQED/QEDalpha; M. Senami, T. Miyazato, S. Takada, Y. Ikeda, and A. Tachibana, J. Phys.: Conf. Ser. **454**, 012052 (2013); M. Senami, Y. Ogiso, T. Miyazato, F. Yoshino, Y. Ikeda, and A. Tachibana, Trans. Mat. Res. Soc. Jpn. **38**(4), 535 (2013); K. Ichikawa, M. Fukuda, and A. Tachibana, Int. J. Quant. Chem. **113**, 190 (2013); K. Ichikawa, M. Fukuda, A. Tachibana, M. Senami, S. Takada, and A. Tachibana, JPS Conf. Proc. **1**, 016014 (2014); M. Fukuda, K. Naito, K. Ichikawa, and A. Tachibana, Int. J. Quant. Chem. **116**, 932 (2016).

[6]For example, see, A. Tachibana, *New Aspects of Quantum Electrodynamics*, Springer (2017).

[7]A. Tachibana, In *Fundamental World of Quantum Chemistry, A Tribute to the Memory of Per-Olov Löwdin*, E. J. Brändas and E. S. Kryachko, Eds, Kluwer Academic, Dordrecht, 2003, Vol. 2, p. 211; A. Tachibana, J. Mol. Modeling **11**, 301 (2005); J. Mol. Struct. (THEOCHEM) **943**, 138 (2010).

[8]K. Doi, Y. Mikazuki, S. Sugino, T. Doi, P. Szarek, M. Senami, K. Shiraishi, H. Iwai, N. Umezawa, T. Chikyo, K. Yamada, and A. Tachibana, Jpn. J. Appl. Phys. **47**, 205 (2008); P. Szarek, Ph.D. dissertation, Kyoto University, 2008; A. Fukushima, Y. Tsuchida, M. Senami, and A. Tachibana, Jpn. J. Appl. Phys. **49**, 111504 (2010); A. Fukushima, S. Sugino, Y. Tsuchida, M. Senami, and A. Tachibana, *ibid.* **49**, 121504 (2010); M. Senami, Y. Tsuchida, A. Fukushima, Y. Ikeda, and A. Tachibana, *ibid.* **51**, 031101 (2012).

[9]M. Senami, Y. Ikeda, and A. Tachibana, Jpn. J. Appl. Phys. **50**, 010103 (2011).

[10]Y. Ikeda, M. Senami, and A. Tachibana, AIP Advances **2**, 042168 (2012).

[11]T. Hara, M. Senami, and A. Tachibana, Phys. Lett. A **376**, 1434 (2012); M. Fukuda, M. Senami, and A. Tachibana, In *Advances in Quantum Methods*

and Applications in Chemistry, Physics, and Biology Progress in Theoretical Chemistry and Physics, Vol. 27, Chap. 7, pp 131–139, Eds by M. Hotokka, E. J. Brändas, J. Maruani, and G. Delgado-Barrio (Springer, New York, 2013); M. Fukuda, K. Soga, M. Senami, and A. Tachibana, Int. J. Quant. Chem **116**, 920 (2016).

[12]Y. Kikuchi, C. Tamura, R. Hasunuma, and K. Yamabe, presented at *Gate Stack Technology and Physics* (2011).

[13]J. Schwinger, J. Math. Phys. **2**, 407 (1961); L. V. Keldysh, Sov. Phys. JETP **20**, 1018 (1965); C. Caroli, R. Combescot, P. Nozieres, and D. Saint-James, J. Phys. C **4**, 916 (1971).

[14]See also, and references therein, S. Datta, *Electronic Transport in Mesoscopic Systems* (Cambridge University Press, New York, 1997); S. Datta, *Quantum Transport: Atom to Transistor* (Cambridge University Press, New York, 2005).

[15]T. Ozaki, Phys. Rev. B **67**, 155108 (2003); T. Ozaki and H. Kino, *ibid.* **69**, 195113 (2004); **72**, 045121 (2005); OpenMX 3.8, http://www.openmx-square.org/.

[16]M. Senami, Y. Ikeda, A. Fukushima, and A. Tachibana, Jpn. J. Appl. Phys. **49**, 115002 (2010).

[17]T. Ozaki, K. Nishio, and H. Kino, Phys. Rev. B **81**, 035116 (2010).